Picometer-Scale Dynamical X-Ray Imaging of Single DNA Molecules

Yuji C. Sasaki,[1,2,*] Yasuaki Okumura,[3] Shinichi Adachi,[4] Hitoshi Suda,[5] Yoshio Taniguchi,[3] and Naoto Yagi[1]

[1]*Biomedical Group, Japan Synchrotron Radiation Research Institute, SPring-8, Mikazuki, Hyogo 679-5198, Japan*

[2]*Unit Process and Combined Circuit, PRESTO, Japan Science and Technology Corporation (JST), Osaka 560-0082, Japan*

[3]*Faculty of Textile Science & Technology, Shinshu University, Ueda, Nagano 386-8567, Japan*

[4]*The Institute of Physical and Chemical Research (RIKEN), Mikazuki, Hyogo 679-5143, Japan*

[5]*Department of Biological Science and Technology, Tokai University, Numazu, Shizuoka 410-0321, Japan*

(Received 20 February 2001; published 26 November 2001)

Time-resolved dynamical x-ray imaging of individual DNA molecules with picometer-scale precision is demonstrated for the first time. Diffracted x-ray tracking (DXT), a single-molecule experiment with x rays, monitors the rotating motions, rather than the translational motions, of a labeled nanocrystal. DXT can obtain information about the dynamics of single molecules through a quantitative analysis, since the signals from DXT are independent of the chemical conditions.

DOI: 10.1103/PhysRevLett.87.248102 PACS numbers: 87.64.–t, 07.85.Qe, 61.10.–i

Imaging methodologies in cell biology ultimately involve both ultrafast time resolution and *in vivo* observations of the structural changes in single biomolecules with atomic-scale precision. For the ultrafast time resolution, ultrashort pulsed sources need to be generated [1–3]. With x rays, free-electron laser-type hard x-ray sources are used to estimate the potential for imaging single protein molecules and small assemblies [4–6]. At the visible light wavelength λ, *in vivo* observations have greatly progressed due to the remarkable development of fluorescence single-molecule detection techniques [7,8]. These single-molecule techniques have been providing positional information at an accuracy of about $\lambda/100$, far below the optical diffraction limit ($\sim\lambda/2$) [7]. We earlier achieved time-resolved x-ray ($\lambda_{\mathrm{x\ ray}} \sim 0.1$ nm) observations of picometer-scale ($\lambda_{\mathrm{x\ ray}}/100$) slow Brownian motions in individual DNA (18-mer) molecules in various aqueous solutions. These dynamical observations of individual single biological molecules are promising for both *in vivo* single-molecular imaging with picometer-scale precision and radiation damage studies on single biomolecules on ultrafast time scales.

In order to detect intramolecular Brownian motions in individual single biological molecules on the picometer scale, we utilized individual diffraction spots from a nanocrystal, which was tightly linked to the DNA molecules under observation [Fig. 1(i)]. In this study, we observed single DNA (18-mer) molecules. Diffracted x-ray tracking (DXT) [9], a single-molecule experiment with x rays, was used to monitor the rotating motions, rather than the translational motions, of the labeled nanocrystal. Random rotational Brownian motions are regarded as Brownian motions on a two-dimensional flat surface. Therefore, the rotational angle [$= \Delta(2\theta)$] of the labeled nanocrystal can be converted to the displacement ($= \Delta z$) at the edge of the observed molecules by $L\Delta(2\theta)/2 = \Delta z$, where L is the length of the observed molecules. To distinguish individual nanocrystals in the image, the spots from the nanocrystals must not overlap, and the number of nanocrystals must coincide with the number of diffracted spots. In consideration of this, we used one-dimensional (Si/Mo) nanocrystals, and the number of diffracted spots from the one-dimensional nanocrystals had to be very small.

In single-molecular detection, it is not important to observe a two- or three-dimensional "image," but rather to continuously determine the center position of the single spot under observation. Therefore, the detection limit of the observed displacements in DXT is only dependent on the accuracy and stability of the observed diffraction angles. In order to measure the total stability of the DXT

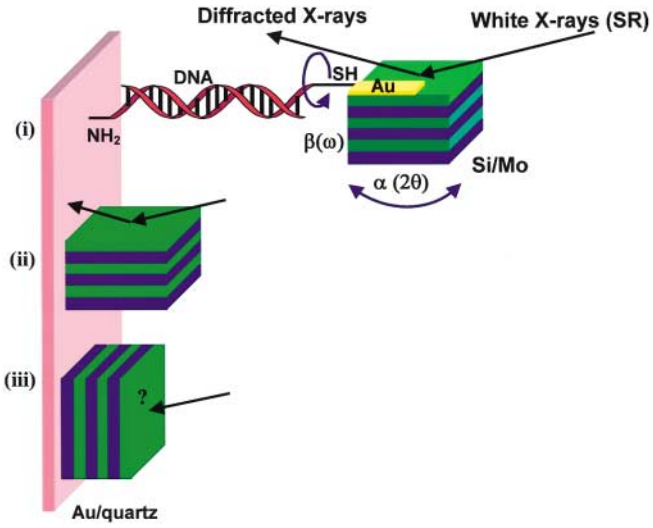

FIG. 1 (color). (i) Schematic drawing of the x-ray single-molecular detection system for individual DNA molecules in aqueous solutions (not to scale). DXT traces the displacement of the single diffracted x-ray spot from the one-dimensional Si/Mo nanocrystal [9], which is linked to the individual DNA molecules. The diameters of the nanocrystal and the DNA molecule are about 30 nm and 2.5–3 nm, respectively. (ii) Schematic drawing of the sample of physical adsorbed Si/Mo nanocrystals on the Au/quartz. (iii) Diffraction spots cannot be monitored when the direction of the stacking period of the Si/Mo multilayer is parallel to the surface of the Au/quartz.

system, we observed the stopped diffraction spots from physical adsorbed nanocrystals [Fig. 1(ii)] on Au/quartz under dry conditions. [This is equivalent to the measurement of the detection limit ($\Delta 2\theta_{\text{limit}}$) in DXT.] Figure 2(i) shows a diffraction spot from a physical adsorbed nanocrystal. We confirmed that the measurements of the diffraction angles (2θ) from the physical adsorbed nanocrystal on the substrate were stabilized within ($\Delta 2\theta_{\text{limit}} =$) 1.5 mrad during 1 s. DXT could monitor $\Delta z_{\text{limit}} = 4.5$ pm when the nanocrystal was tightly coupled to the DNA molecule under observation ($L_{\text{DNA}} =$ 6 nm), since the limited displacement Δz_{limit} in this DNA system was expressed by $\Delta z_{\text{limit}} = 0.75 \times 10^{-3} L$. Figure 2(ii) shows a histogram of intensities of individual diffracted spots. Each single diffracted x-ray spot was quantized at about 500 counts per 3 ms. This shows that DXT can quantitatively measure x-ray intensities from single nanocrystals [9], since the signals from DXT are independent of chemical conditions.

We used multilayer-(Si/Mo)-nanocrystals, because many nanocrystals are not perfectly crystallized. The number of diffracted spots from the multilayer-nanocrystals enabled us to determine the number of observed nanocrystals, since a diffracted x-ray spot was only reflected from a single multilayer-nanocrystal. We chose both the lattice constants and stacking period ($d = 5$ nm, 4 pairs) for Si/Mo. In order to achieve reactions with thiol groups at the end of the observed DNA, we deposited a Au thin film (5 nm) on the surface of the Si/Mo multilayer by vacuum evaporation. Therefore, the total Si/Mo thickness (the vertical size) was 25 nm. We confirmed this total thickness value by electron scanning microscopy (SEM, *S*-5000, Hitachi, Ltd.) and x-ray reflectometry. The Si/Mo nanocrystals were fabricated by a sequential process using a silicon substrate, silicon dioxide beads, and microprocessing techniques including reactive ion etching [9]. We confirmed that the averaged diameter (the horizontal size) of the Si/Mo one-dimensional nanocrystal was about 30 nm by SEM. We also confirmed that there were no diffracted spots from the deposited Au film on both the quartz substrate and the nanocrystals, because the Au film was amorphous and not crystalline. Unfortunately, we were not able to monitor a Si/Mo one-dimensional nanocrystal of the same size as that fabricated by the microprocessing techniques of our previous work [9]. In this work, however, we did succeed in fabricating high reflective Si/Mo nanocrystals by decreasing the roughness in the interface of the Si/Mo multilayer [10].

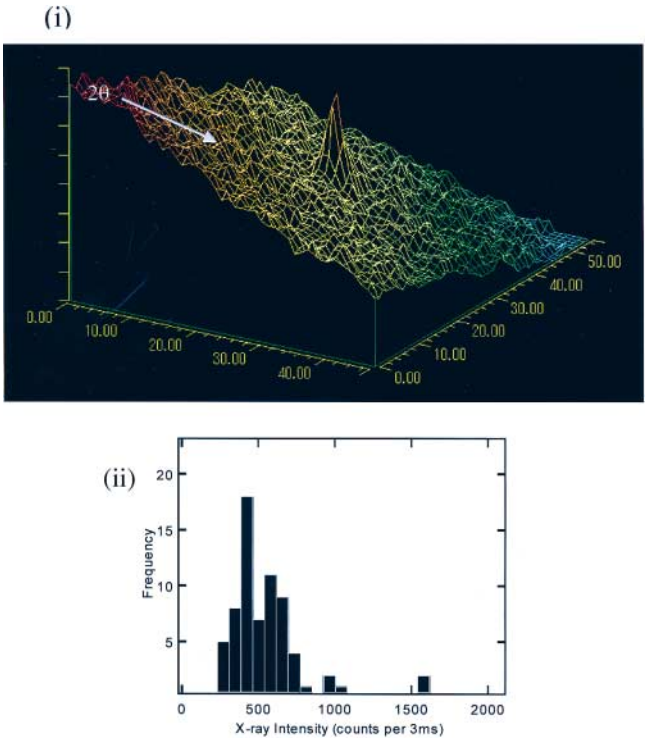

FIG. 2 (color). (i) Three-dimensional image of the observed single diffraction spot from the physical adsorbed one-dimensional nanocrystal on the Au/quartz substrate. The units in the x and y axis are pixel (50×50 pixel^2). The averaged x-ray intensity of this spot is about 500 per 3 ms. We can determine the center position of the observed spot at an accuracy of one pixel. (ii) Histogram of peak intensity of observed diffraction spots.

In order to react a single DNA molecule with a single nanocrystal, we restricted the size of the reactive area in the Si/Mo nanocrystal. Strictly speaking, the form of such a nanocrystal depends not on the column but on the cone because of the over-etching process. We confirmed that the upper and lower diameters of the cone were about 10 and 40 nm, respectively, by SEM. Therefore, a decrease of the reactive area, which is the upper Au surface of the conical Si/Mo nanocrystal, enables the reaction between a single nanocrystal and a single DNA molecule.

The DNA sequences were 5′-*SH-CAGTCAGGCAGTCAGTCA*-3′ and 5′-NH2-*TGACTGACTGCCT GACTG*-3′ [11]. We first used the chemical coupling made between the amino groups (NH2) at the end of the DNA (100 μl, 0.1 nM/mL) and the surface of the evaporated Au thin film on the quartz (Au/quartz, 10×10 mm) by a cross-linking reagent (SPDP, Dojindo Lab.) in 50 mM tris/HCl (pH = 8.0) for 12 h at 4 °C. The chemical reaction between the amino groups in the DNA molecule and the cross-linking reagent started after the surface of the evaporated Au thin film on the quartz became saturated with the cross-linking reagent [SPDP (1 mM)] in N, N-dimethylformamide (DMF) for 12 h at 4 °C. Because of this, the thiol groups (SH) at the other end of the DNA molecules were unable to react with the surface of the evaporated Au on the quartz substrate. Next, the evaporated Au thin film on the surface of the Si/Mo nanocrystal was coupled to the thiol groups at the end of the DNA in 50 mM MOPS (pH = 7.0) for 6 h at 4 °C. Then, 7 μl of solution (50 mM tris/HCl, pH = 8.0, 4 °C) was mounted on the adsorbed DNA molecules.

When the adsorption efficiency of the DNA molecules on the substrate was about 2%, the estimated density of the adsorbed DNA molecules was expected to be about

900 (about 30 nm × 30 nm) nm^2/molecule. Since this occupied area of the adsorbed DNA molecules was in approximate agreement with the geometric size of the Si/Mo one-dimensional nanocrystal, the single nanocrystal was expected to react with a single DNA molecule. In general, the adsorption efficiency of molecules on such a surface is less than 1% [12,13]. We confirmed that the average density of Si/Mo one-dimensional nanocrystals was about 4000 (about 63 nm × 63 nm) nm^2/nanocrystal by SEM.

Here, we discuss the effects of labeled nanocrystals. The nanometer-level analysis [called single particle tracking (SPT) [14,15]] of movements of membranes with gold nanoparticles was demonstrated for the first time in 1985–1988. Ever since then, there have been a lot of discussions about the effects of labeled small particles [16]. As a result, many researchers have concluded that analyses by using labeled nanoparticles can provide significant information about biological events [17,18]. In addition, we confirmed in our previous work [9] that a viscosity below 273 K is able to be determined from DXT data. Because the polymer local chains in beaded agarose gel are labeled with Si/Mo nanocrystals, the dynamics of these local molecules is not affected by labeling nanocrystals. Accordingly, we estimated that the behavior of the labeled DNA molecules in this work would not be dominated by any nanocrystals.

We used the white x-ray mode (Laue mode) of beam line BL44B2 (RIKEN Structural Biology II, SPring-8, Japan) to record Laue diffraction spots from one-dimensional Si/Mo nanocrystals on a Au/quartz (70 μm) substrate. The photon flux at the sample position was estimated to be about 10^{15} photon/sec/mm^2 in the energy range of 7–30 kV. The x-ray beam's focal size was 0.2 mm (horizontal) × 0.2 mm (vertical). A diffraction spot was monitored with an x-ray image intensifier (Hamamatsu Photonics, V5445P) and a CCD camera (Hamamatsu Photonics, C4880-82) with 656 × 494 pixels. The average exposure time was 1 sec. The detector's effective size was 150 mm in diameter with a 150 mm sample-to-detector distance. We calibrated the movements of the observed diffracted spots from the fixed Si/Mo nanocrystals on the sample holder when the goniometer was moved during $2\theta = 0$–500 mrad.

Figure 3(i) shows movements of diffracted angles θ from a single nanocrystal coupled to a single DNA molecule (18-mer) at 4 °C. The motions of diffracted spots can be clearly distinguished between the direction of diffraction angles θ and circumference ω in Fig. 1. In the figure, the motions of θ and ω are in accord with those of adsorbed DNA molecules in real space (modes α and β, respectively, in Fig. 3). It is known that motions consistent with the β degree of freedom lead to radial displacement ω of a diffraction spot on a detector since the lattice spacing presented to the x-ray beam does not change for these motions, while for the α degrees of freedom the lattice spacing presented to the x-ray beam changes and leads to a different value for 2θ. The observed spots randomly

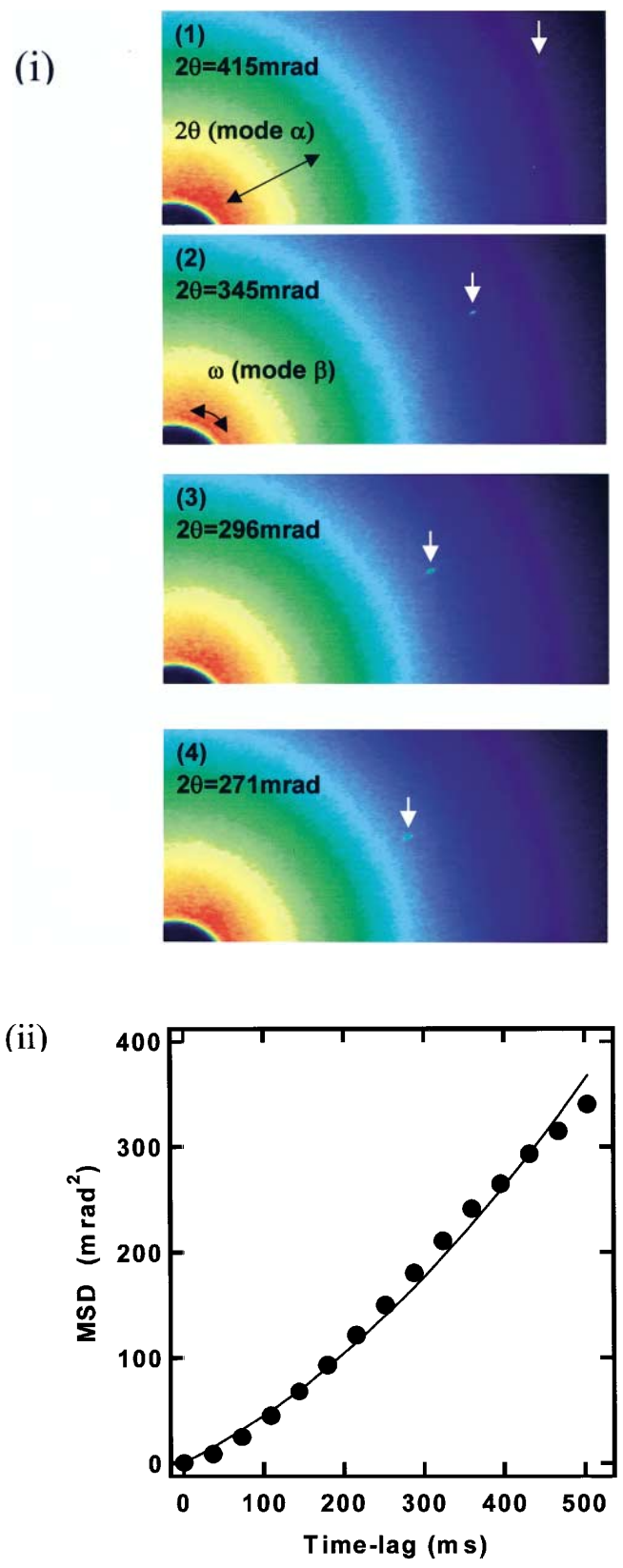

FIG. 3 (color). (i) Examples of the diffracted spots from the single Si/Mo nanocrystal in aqueous solutions appeared as brightly shining dots (white-blue). Frames are spaced at 180-ms intervals. The exposure time was 1 s. (ii) MSD $\langle \Delta\theta^2 \rangle$ as a function of time interval Δt. These data were obtained from about 60 diffracted spots.

move along the direction of θ, and there is no displacement of the diffracted spots along the direction of ω. This indicates that the nanocrystal is tightly coupled to the observed DNA molecule, and that the main motion of the nanocrystal is assigned to mode α.

In a simple Brownian diffusion, the $(\Delta\theta^2)$-Δt plots are linear with a slope of $4D$, where $(\Delta\theta^2)$ is the mean square displacement of the observed spots, Δt is the time interval, and D is the two-dimensional diffusion coefficient. The simple diffusion mode can be expressed as $(\Delta\theta^2)L^2 = 4D(\Delta t)$. However, from the relationship between $(\Delta\theta^2)$ and Δt [Fig. 3(ii)], the observed displacement of θ is assigned as directed by the Brownian movement [9,16]. This relationship is known as the directed diffusion mode: $(\Delta\theta^2)L^2 = 4D(\Delta t) + v^2(\Delta t)^2$. This shows that nanocrystals move in a direction at a constant drift velocity v with a diffusion coefficient of D. Since the values of D and v can be used to analyze Brownian motions, these parameters (D and v) are physically important ones. From these values, Brownian motions are classified as follows: Brownian motions and non-Brownian motions [16]. In addition, the physical dominant factor on single-molecular scales under solution systems is not the mass (weight) but the viscosity. The relative viscosity can be estimated from the value of D through the Einstein-Stokes-law [16]. If we observe local values of D in all single molecules by using data from the different positions of the labeled nanocrystals, we can discuss not the absolute values of viscosities but the relative values. Moreover, we may be able to obtain information about the kinetics and structures of the individual single molecules by using our DXT.

From the curve fitting, we obtained the values of the diffusion constant $D = 95 \pm 12$ mrad^2/s and the constant drift velocity $v = 26 \pm 8$ mrad/s. The observed parabolic MSD curve showed that there is no steric inhibitor to the motions of the adsorbed DNA molecules in this system. If there were steric restricted motions of the adsorbed DNA molecules due to the presence of the substrate surface or the adsorbed Si/Mo nanocrystal, the relationship between $\langle\Delta\theta^2\rangle$ of the diffracted spots and Δt would have shown an asymptotic curve [16].

Radiation damage was caused by x-ray photons depositing energy into the sample system. We confirmed the reproducibility of the data up to an exposure time of 3 s. At exposure times above 4 s, the motions of the nanocrystals stopped or slowed down. Although it was difficult to determine the origin of the radiation damage, we can say that the modification of the observed motions may have been influenced not by the radiation effect of the DNA molecules, but by the ionization of the nanocrystals, which consisted of heavier elements than those of the DNA molecules. In addition, the nanocrystals were larger than the DNA molecules. On the other hand, we confirmed the presence of a constant drift in the solution from the obtained MSD curve. This may have caused the observed local rise in the temperature of the solution due to radiation.

In the future, the biggest challenge will be to observe individual and rare biological processes in living cells. DXT can be used to monitor not translational motions but orientational ones on picometer scales. DXT can be expected to observe the structural changes accompanying the activation of ion channels in living cells. Such changes are known as tilting or small orientational motions of the helix in channel pores [8,19]. DXT can also be expected to monitor the dynamics of the ion channels through ionic flux measurements by the patch-clamp technique. At present, some groups are trying to observe the dynamics of ion channels by using single-molecular fluorescence techniques. Unfortunately, it has been very difficult to observe structural changes because of the lack of a sufficient monitoring precision.

We thank the staff of Tokyo Electronics and Mechanics Co. and of Dojindo Lab. for technical support. The synchrotron radiation experiments were performed at the SPring-8 with the approval of the Japan Synchrotron Radiation Research Institute (JASRI) (Proposal No. 1999B0019-CL-np).

*To whom all correspondence and requests for materials should be addressed.
Email address: ycsasaki@spring8.or.jp

[1] C. Rischel *et al.,* Nature (London) **390**, 490 (1997).
[2] C. Rose-Petruck *et al.,* Nature (London) **398**, 310 (1999).
[3] H. Ihee *et al.,* Science **291**, 458 (2001).
[4] R. Neutze *et al.,* Nature (London) **406**, 752 (2000).
[5] M. Tegze *et al.,* Nature (London) **407**, 38 (2000).
[6] J. Jiao, P. Charalambous, J. Kirz, and D. Sayre, Nature (London) **400**, 342 (1999).
[7] W. E. Moerner and M. Orrit, Science **283**, 1670 (1999).
[8] S. Weiss, Science **283**, 1676 (1999).
[9] Y. C. Sasaki *et al.,* Phys. Rev. E **62**, 3843 (2000).
[10] Y. Okumura, Y. C. Sasaki, and Y. Taniguchi, Phys. Rev. B (to be published).
[11] A. P. Alivisatos *et al.,* Nature (London) **382**, 609 (1996).
[12] H. Suda *et al.,* Biochem. Biophys. Res. Commun. **261**, 276 (1999).
[13] Y. C. Sasaki *et al.,* Biophys. J. **72**, 1842 (1997).
[14] M. De Brabander *et al.,* Cytobios **43**, 273 (1985).
[15] J. Gelles, B. J. Schnapp, and M. P. Sheetz, Nature (London) **331**, 450 (1988).
[16] M. J. Saxton and K. Jacobson, Annu. Rev. Biophys. Biomol. Struct. **26**, 373 (1997).
[17] Y. Harada *et al.,* Nature (London) **409**, 113 (2001).
[18] R. Yasuda *et al.,* Nature (London) **410**, 898 (2001).
[19] E. Perozo, D. M. Cortes, and L. G. Cuello, Science **285**, 73 (1999).